


RESEARCH ARTICLE

Miniature and cost-effective self-powered triboelectric sensing system toward rapid detection of puerarin concentration

Chang Su^{1,2} | Jiajia Shao^{1,3} | Zeyang Yu^{1,3} | Al Mahadi Hasan¹ |
Chengmin Bao^{1,2} | Chris R. Bowen⁴ | Chuanbo Li² | Zhong Lin Wang^{1,5,6} |
Ya Yang^{1,3} 

¹Beijing Key Laboratory of Micro-nano Energy and Sensor, Center for High-Entropy Energy and Systems, Beijing Institute of Nanoenergy and Nanosystems, Chinese Academy of Sciences, Beijing, People's Republic of China

²College of Life and Environmental Sciences, College of Science, Optoelectronic Research Center, Minzu University of China, Beijing, People's Republic of China

³School of Nanoscience and Technology, University of Chinese Academy of Sciences, Beijing, People's Republic of China

⁴Department of Mechanical Engineering, University of Bath, Bath, UK

⁵School of Material Science and Engineering, Georgia Institute of Technology, Atlanta, Georgia, USA

⁶Yonsei Frontier Lab, Yonsei University, Seoul, Republic of Korea

Correspondence

Chuanbo Li, College of Life and Environmental Sciences, College of Science, Optoelectronic Research Center, Minzu University of China, Beijing 100081, People's Republic of China.
Email: cbli@muc.edu.cn

Zhong Lin Wang and Ya Yang, Beijing Key Laboratory of Micro-nano Energy and Sensor, Center for High-Entropy Energy and Systems, Beijing Institute of Nanoenergy and Nanosystems, Chinese Academy of Sciences, Beijing 101400, People's Republic of China.
Email: zhong.wang@mse.gatech.edu and yayang@binn.cas.cn

Funding information

National Key R & D Project from Minister of Science and Technology in China, Grant/Award Number: 2021YFA1201604; National Natural Science Foundation of China, Grant/Award Number: 52072041; Beijing Natural Science Foundation, Grant/Award Number: JQ21007

Abstract

The detection of puerarin concentration is an essential capability to study the functional role of the Pueraria root as a natural medicine and dietary source in the treatment of cardiovascular diseases and liver protection. Current methods to detect and measure puerarin concentration, such as ultraviolet–visible spectrophotometry (UV), are bulky, require an external power supply, and are inconvenient to use. Here, we propose a triboelectric puerarin-detecting sensor (TPDS) which is based on liquid–solid contact electrification, in which liquid–solid interactions generate rapid electrical signals in only 0.4 ms to enable real-time detection of puerarin concentration in water droplets. The electrical signal of the TPDS decreases with an increase of puerarin concentration, and the sensitivity of the approach is $520 \text{ V} \cdot (\mu\text{g/mL})^{-1}$. The TPDS represents a miniature and cost-effective sensor that is 0.2% of the size and 0.01% of the cost of a UV spectrophotometer. Our theoretical analysis verified that the puerarin concentration in droplets can effectively regulate the electronic structure, where higher concentrations of puerarin lead to a narrower energy bandgap, which allows the TPDS to detect puerarin concentration without the need for an external power supply. The TPDS therefore provides a route for the

Chang Su and Jiajia Shao contributed equally to this work.

This is an open access article under the terms of the [Creative Commons Attribution](https://creativecommons.org/licenses/by/4.0/) License, which permits use, distribution and reproduction in any medium, provided the original work is properly cited.

© 2024 The Author(s). *InfoMat* published by UESTC and John Wiley & Sons Australia, Ltd.

development of a portable and self-powered method to measure the concentration of an active ingredient in droplets through the conversion of natural energy.

KEYWORDS

concentration detection, density functional theory, puerarin, self-powered, triboelectric sensor

1 | INTRODUCTION

The accumulation of active ingredients in natural medicines is influenced by their place of origin, harvesting method, and processing methods employed,¹ which subsequently affects their efficacy for treating diseases.² Therefore, real-time monitoring of the content of active ingredients is particularly important for process optimization and enhancing the effectiveness of natural medicines. Pueraria root, derived from the Leguminosae plant *Pueraria lobata* (Wild.) Ohwi, is well-known both as a herbal medicine and a food source, where there are abundant species and resources in Asia, America, and Europe.^{3–5} It has been traditionally used to treat diabetes, hypertension, hyperlipidemia, diarrhea, and fever,⁶ while also being rich in nutrition and suitable for enhancing human immunity through a variety of delicious foods.^{7,8} Pueraria root has demonstrated notable efficacy with minimal adverse reactions. The effects of treating hypertension and decomposing alcohol are largely attributed to the presence of isoflavones,^{9–14} with the main isoflavone compounds found in Pueraria root being puerarin.^{15,16} Therefore, the concentration of puerarin serves as an indicator of the efficacy of Pueraria root in treating human diseases. Common methods for extracting puerarin from *P. lobata*, such as boiling and ultrasonic extraction, have long extraction and heating times and can cause damage to certain components.^{17–22} The most commonly employed techniques for quantifying puerarin concentration encompass chromatography and spectrometry, as exemplified by high-performance liquid chromatography (HPLC) and ultraviolet–visible spectrophotometry (UV–Vis spectrophotometry), respectively. However, these methods require the use of bulky and expensive instruments, as well as highly skilled operators for sample handling and analysis. These include the use of fine filter membranes for the removal of impurities in the preparation process of samples and the consumption of mobile phases in the analytical process. In addition, HPLC and other instruments are only able to be used using a single column, which restricts their ability to analyze multiple samples simultaneously. The time-consuming pretreatment process not only necessitates

the involvement of professional technicians, but also constrains the real-time detection of puerarin. Consequently, there is a pressing need for the development of a novel instrument that can facilitate the real-time detection of puerarin in a rapid, cost-effective, and lightweight manner.

In this regard, an electrical signal may be generated from the contact or friction of two materials, and triboelectric nanogenerators (TENGs) are constructed based on this phenomenon, which operate based on a minimal driving force. Such devices can gather mechanical energy and convert it into electrical energy.^{23,24} The TENG is characterized by a high sensitivity, rapid response time, lightweight nature, and low cost. As a result, it is an ideal solution for the providing potential portability and overcoming the challenge of existing large and heavy content-determination instruments. In addition, previous research has successfully identified liquids with the aid of a TENG,²⁵ where the study devised a triboelectric droplet-tasting sensor that employs morphological alterations of droplets and variations in electrical signals to identify the liquid type. Hence, the analysis of electrical signals generated by liquid–solid friction may enable the detection of liquid concentration.

Here, we have developed a triboelectric puerarin-detecting sensor (TPDS). The TPDS comprises of an upper electrode, a fluorinated ethylene propylene (FEP) friction layer, a Kapton dielectric layer, and a lower electrode that captures the energy from the liquid–solid contact. The sensor operates on the principle that the saturation of friction materials affects electron transfer, making it possible to rapidly detect the concentration of puerarin without the need for an external power source. The TPDS device has a volume of 125 cm³ and a low cost of \$1.4. In comparison to ultraviolet–visible spectrophotometry, it utilizes only 0.2% of the volume and 0.01% of the cost. Furthermore, the TPDS can be self-powered and has a response time of only 0.4 ms. As a result, this sensor solves the issues associated with large volumes and high costs in determining concentration. Our density functional theorem (DFT) calculations reveal that when water-solubilized puerarin makes contact with FEP

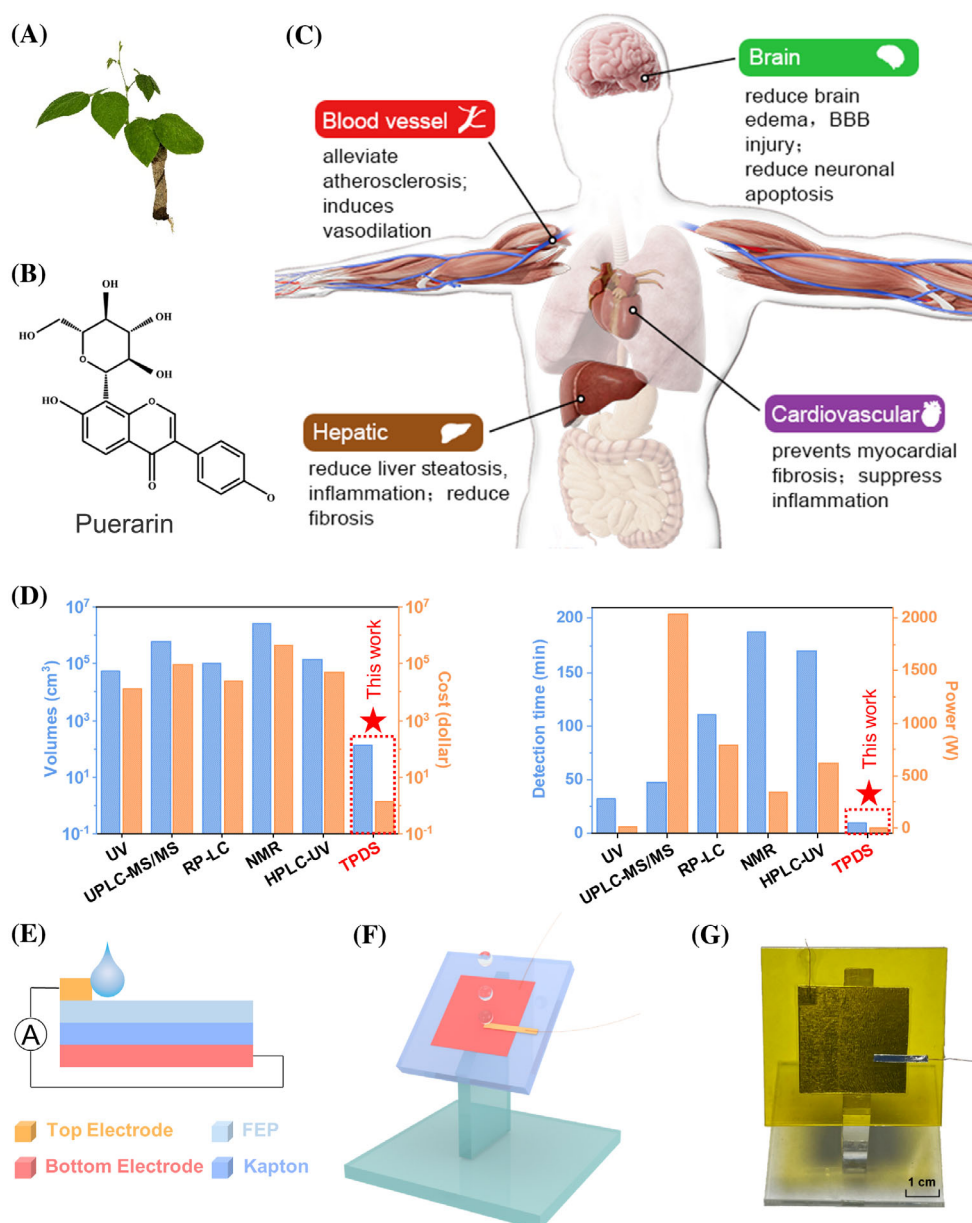


FIGURE 1 Triboelectric puerarin-detecting sensor (TPDS) for determining the content of puerarin in *P. lobata*. (A) Overall plant map of *P. lobata*. (B) Molecular formula of puerarin. (C) Positive effects of puerarin on the human body. (D) Comparison of UV, UPLC-MS/MS, RP-LC, NMR, HPLC-UV, and TPDS in volumes, cost, detection times, and energy consumption. (E) Schematic of TPDS. (F) Model diagram showing droplet contact with TPDS. (G) Picture of the TPDS.

incorporating more puerarin molecules into the solution diminishes the number of electrons transmitted from the water to the FEP. The phenomenon may be associated with the greatest energy of the largest highest occupied molecular orbital (HOMO) energy and the lowest unoccupied molecular orbital (LUMO) energy. This study provides a new understanding of the liquid–solid contact mechanism utilized in component concentration detection and offers valuable insights into the development a user-friendly content determination methods and models.

2 | RESULTS AND DISCUSSION

2.1 | Miniature and cost-effective self-powered TPDS can reduce detection time

In this work, we developed a TPDS that can detect the flavonoid content of *P. lobata* (Figure 1A), such as puerarin (Figure 1B). It is particularly important to be able to determine the concentration of puerarin because of its ability to alleviate atherosclerosis and induce vasodilation, reduce the degree of hepatic steatosis, inflammation and fibrotic

liver damage, and prevent cardiovascular and blood–brain barrier (BBB) lowering; see Figure 1C.^{26–28} Compared to current methods, such as ultraviolet–visible spectrophotometry (UV), ultra-performance liquid chromatography/tandem mass spectrometry (UPLC-MS/MS) and reversed-phase liquid chromatography (RP-LC),⁹ quadruple proton nuclear magnetic resonance (NMR) and high-performance liquid chromatography with ultraviolet detection (HPLC-UV), TPDS collects the energy in the droplet and detects the amount of drug in the droplet in a low-cost, small-volume, and rapid manner (Figure 1D).^{9,29–31} The UV-based method has the smallest volume of any previous measurement method at 54 720 cm³, while the TPDS has a volume of only 125 cm³ or 0.2% of UV method volume. While UV has the lowest cost of the current available methods at \$12 555, the TPDS approach has a cost of only \$1.4, a reduction of four orders of magnitude, or 0.01% of UV's cost. The TPDS has an inspection time of only 9 min, including 8 min for an extraction test; see Table S1.

The structure of the TPDS is shown in Figure 1E. As the droplet falls, it comes into contact with the upper electrode and makes contact against the FEP friction layer (Figure S1A), thereby generating an electrical signal as an output. The Kapton acts as a dielectric layer that increases the charge storage and enhances the electrical signal (Figure S1B,C). During operation, the TPDS is tilted at 45°, as in Figure 1F, and the droplet slides down by gravity, and a cyclic process is completed. A tilt of 45° facilitates droplet slippage and has been demonstrated to yield the most optimal results when compared to other tilting angles (Figure S2). The TPDS provides a low-cost, small-volume method to rapidly detect the concentration of puerarin in the droplet. An overall illustration of the TPDS is shown in Figure 1G.

The electrical signal for detecting pure water with the TPDS leads to an open-circuit voltage of 109 V and a short-circuit current of 28 µA (Figure S3). In general, the output power (P) can be calculated from the external load resistance by,

$$P = I^2 R$$

where I is the current and R is the load resistance. Finally, we can obtain the maximum power of the TPDS as 1429 µW (Figure S3).

2.2 | TPDS to detect puerarin solution brewed under different conditions

The TPDS was used to detect the effects of extraction temperature, solid–liquid ratio, and extraction time on the efficiency of hot water extraction of Pueraria root

(Figure 2A). To ensure the accuracy of the TPDS, the concentration of Puerarin was simultaneously determined using UV spectrophotometry. The extracted solution was diluted in a 1:100 gradient and added dropwise to the FEP friction layer of the TPDS, thereby generating electrical signals of different values. The dissolution of puerarin from Pueraria root increased with increasing extraction temperature (Figure 2B). The results for the TPDS showed that the magnitude of the current and voltage signals decreased with increasing extraction temperature, which was inversely proportional to the concentration of puerarin in the solution. Similarly, the magnitude of the electrical signals detected by TPDS were inversely proportional to the content of puerarin in solution as the solid–liquid ratio and extraction time varied. The experimental results showed that the highest solubility of puerarin was obtained when the extraction temperature was 100°C (Figure 2B). A decrease in the solid–liquid ratio to 1:30 resulted in a deceleration of the decline in puerarin concentration (Figure 2C). At a solid–liquid ratio of 1:50, the puerarin concentration in the solution reached its minimum, and the solubility of puerarin was greatest after an extraction time of 8 min (Figure 2D).

The absorbance of the Pueraria root solution was determined using UV spectrophotometer using an external standard method. The concentration of puerarin was calculated as follows:

$$c = A/\epsilon l.$$

Here A represents the absorbance, ϵ represents the molar extinction coefficient, and l represents the thickness of the solution. The puerarin demonstrated excellent linearity in the concentration range of 0–50 µg mL⁻¹ (Figure S4). In addition, the UV spectrophotometer showed high precision, good reproducibility, and stability (Table S2). The recovery results indicated that the method was feasible (Table S3).

2.3 | TPDS to detect the concentration of puerarin in Pueraria root from different origins

Factors such as climate, geological environment, and elemental composition of the soil can lead to differences in the content of puerarin in Pueraria root. As a result, the content of puerarin in a Pueraria root from different production areas can vary. Puerarin was detected by TPDS in Pueraria root from six production areas: Zhangjiajie in Hunan Province (HN-ZJJ), Suizhou in Hubei Province (HB-SZ), Nanning in Guangxi Province (GX-NN),

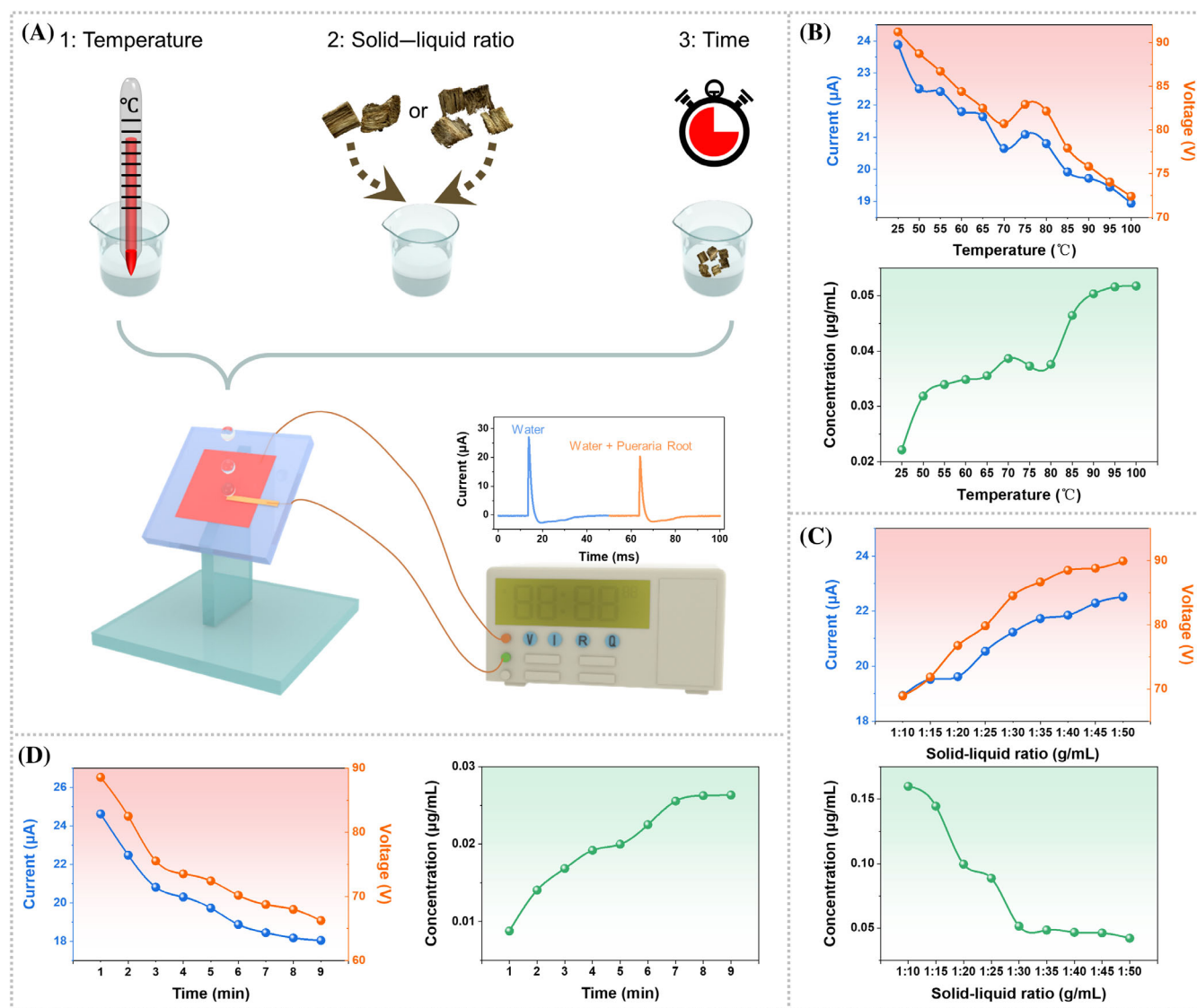


FIGURE 2 Detection of puerarin concentration in solution using TPDS. (A) Schematic of TPDS for detection of puerarin by hot water extraction under extraction temperature, solid-liquid ratio, and extraction time. Illustration displays the current signal of the TPDS to detect the water output and Pueraria root liquid. (B–D) Variation of current, voltage measured by TPDS and puerarin concentration with temperature (B), solid-liquid ratio (C), time (D). Electrical signal detected by TPDS decreased with the puerarin content increased.

Shangluo in Shaanxi Province (SX-SL), Chengdu in Sichuan Province (SC-CD) and Jinzhai in Anhui Province (AH-JZ); see Figure S5. The results showed that the electrical signals detected by TPDS were different (Figures S4 and S5), with the largest electrical signals from region AH-JZ and the smallest electrical signals from region SC-CD (Figure 3A). The concentration of Pueraria root was detected by UV spectrophotometer, and the results showed that SC-CD had the highest concentration of Pueraria root and AH-JZ had the lowest (Figure 3B), indicating that the size of the electrical signals detected by TPDS was inversely proportional to the concentration of Pueraria root. The electrical signals were detected by TPDS after diluting the solutions of Pueraria root from

the six production regions in different gradients (Figure 3C). The results showed that the electrical signals became weaker as the solution concentration increased. A schematic simulating TPDS detection of the output electrical signals of high and low-concentration solutions showed that the output electrical signals of high-concentration solutions were smaller, indicating that fewer electrons were transferred (Figure 3D). After a droplet is introduced into the TPDS, it spreads out and interacts with the FEP friction surface, generating triboelectricity. The droplet is positively charged, where the higher the puerarin concentration the lower the charge the droplet produces; as the FEP is negatively charged, the positive charge flows from the bottom electrode to

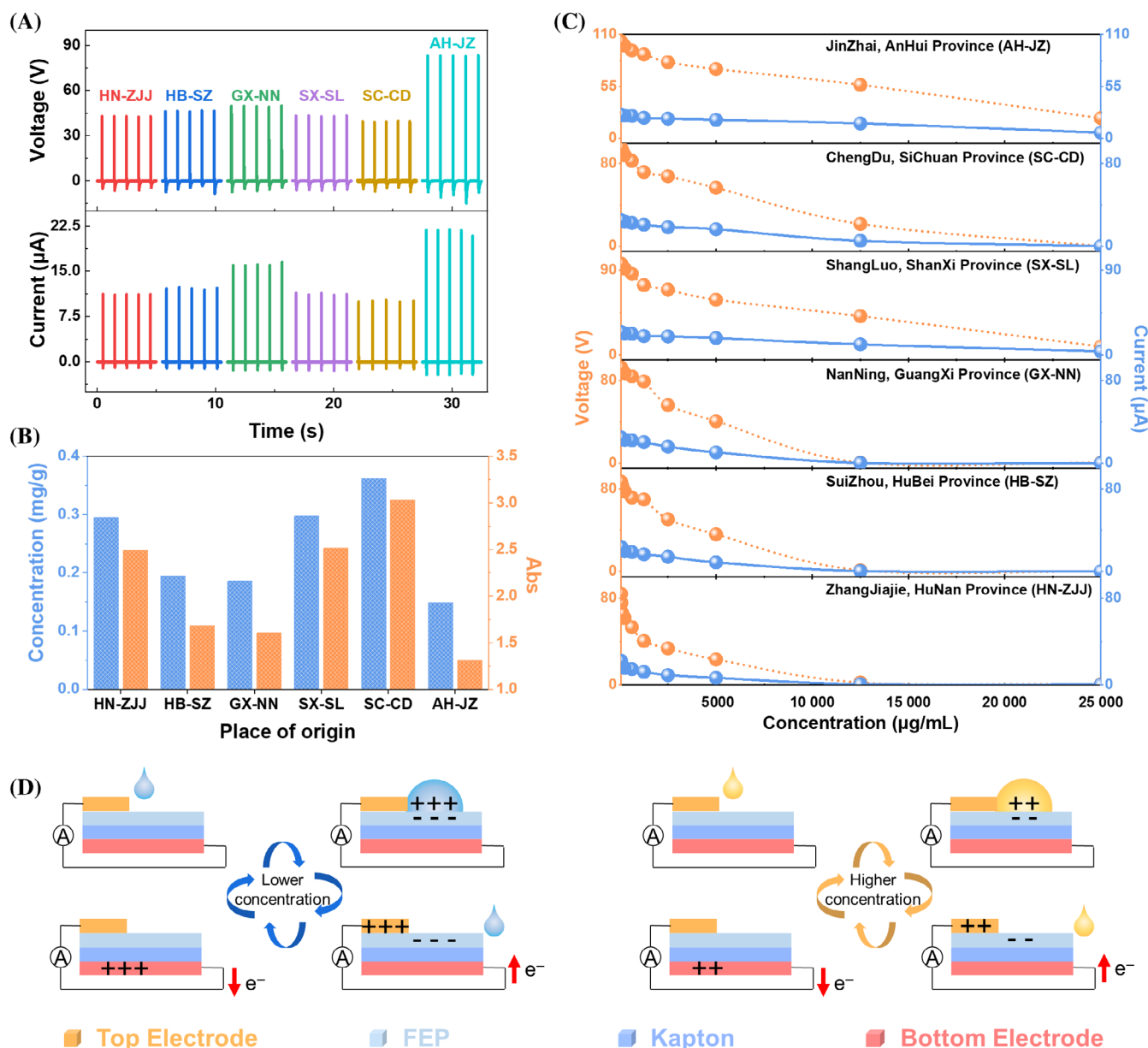


FIGURE 3 TPDS to determine the amount of puerarin in pueraria roots from various regions. (A) Electrical signal diagram for detection of Pueraria root by TPDS. (B) Absorbance and concentration levels of puerarin in Pueraria root brewed solutions from various production areas are compared. (C) Electrical signal diagrams detected by TPDS in different dilution conditions of Pueraria root from distinct production regions are analyzed. Electrical signal generated decreases as the concentration of the solution increases. (D) Schematic of simulating the output electrical signal of high and low concentration puerarin solution. Electrical signal of the lower concentration solution is greater, indicating increased electron transfer.

the top electrode with the objective of neutralizing the negative charge of the FEP. The positive charge generated at the bottom electrode is returned as the droplet flows away from the FEP friction material. The process of generating a current is then repeated as subsequent droplets fall.

In order to investigate the performance of TPDS in detecting the concentration of puerarin, water droplets with a known puerarin concentration were applied onto

the FEP surface, and it was found that the output current and voltage of the droplet decreased with an increase in puerarin concentration (Figure S8), and the electrical signals detected by the TPDS continued to decrease with an increase of puerarin concentration. Figure S8E,F estimates the sensitivity of TPDS by comparing the difference in current (dI) and voltage (dU) as the concentration of puerarin changes (dC), with sensitivities ranging from 3 to 520 $V \cdot (\mu g/mL)^{-1}$ for dU/dC and up to

105 $\mu\text{A} \cdot (\mu\text{g}/\text{mL})^{-1}$ for dI/dC , and the high sensitivities indicate that TPDS has excellent performance. The optimal sensitivity was observed when the concentration range of puerarin was between 0 and 1 $\mu\text{g mL}^{-1}$, and the electrical signals demonstrated discernible differences, even when the concentration range exhibited minimal variation. This phenomenon elucidates the discrepancy between the slight alterations in concentration and the pronounced fluctuations in electrical signals at extraction temperatures of 90–100°C (Figure 2B), solid–liquid ratios of 1:30–1:50 (Figure 2C), and extraction times of 7–9 min (Figure 2D). The elevated sensitivities substantiate the exceptional performance of the TPDS. As shown in Figure S8, the response and recovery times of TPDS are faster than 20 ms, with the fastest being 0.4 ms, which realizes the synchronization between concentration detection and droplet stimulation. In conclusion, the TPDS was employed to ascertain the concentration of puerarin in solution, exhibiting a response time of 0.4 ms and a sensitivity of 520 $\text{V} \cdot (\mu\text{g}/\text{mL})^{-1}$ for puerarin concentrations ranging from 0 to 1 $\mu\text{g mL}^{-1}$.

To assess the durability and reliability of the TPDS, we conducted a 1000-repetition test in which drops of Puerarin-containing droplets were added uninterruptedly. The current signals were recorded throughout the test, and the results demonstrated that the TPDS exhibited consistent performance even after 1000 repetitions (Figure S9). To further investigate the stability of the TPDS, the standard deviation (RSD) of the current change was tested when the TPDS were made after 0 and 180 days. The results demonstrated that the RSD values were 0.836% and 1.665%, respectively, indicating that the sensors exhibited stability and reliability (Table S4).

The pH and contact angle of the solution were determined to investigate the mechanism of TPDS detection of puerarin concentration. The pH of the solutions with different concentrations of puerarin ranged from 6.0 to 6.5 (Figure S10), and the change in pH was not consistent with the trend of the electrical signal; this indicated that there was no direct relationship between the pH of the solution and the magnitude of the electrical signal. The results of the contact angle measurement showed that the contact angle decreased as the concentration of puerarin in the solution increased (Figure S10). The contact area increases as the contact angle decreases, so that as the friction area increases the electrical signal increases if the charge generated by friction per unit area remains unchanged. The experimental results show that the electrical signal is small for a small contact angle, and there is no direct relationship between the concentration of puerarin in TPDS and the contact angle.

2.4 | General theoretical model and understanding of TPDS operation

The charge transfer difference between the FEP friction layer and water is obtained as the concentration of puerarin (PUE) changes (Figure 4A), and the increase and decrease in charges are indicated by the blue and red regions. It is found that the red regions are largely obtained from water, and the blue regions are obtained from FEP, which demonstrates that electrons are transferred from water to the FEP friction layer. However, as the puerarin concentration increases, the number of transferred electrons from water to the FEP decreases. In order to understand the mechanism by which the puerarin can affect electron transfer, we calculated the molecular orbitals of water and different polymers (Figure 4B). The largest highest occupied molecular orbital (HOMO) energy and the lowest unoccupied molecular orbital (LUMO) energy of gap of FEP/ H_2O is approximately 5.72 eV, while the HOMO–LUMO gap of FEP/PUE decreases to 4.22 eV. This result suggests that the number of electrons transferred from water to the FEP friction layer may be proportional to the increase of the HOMO–LUMO gap, which is strongly related to the different functional groups of the polymers. In addition, the electronic structures will be rearranged upon transfer of charges, in order to achieve a new stable state. For example, certain fluorine atoms in FEP can carry a negative charge, while others can carry a positive charge. As observed in Figure 4D,E, oxygen atoms possess a positive charge in FEP/ H_2O , but a negative charge when puerarin is added, due to the presence of distinct functional groups. As the puerarin concentration increases, more electrons are transferred from water to the puerarin, leading to less charges being transferred to the FEP friction layer (Figure 4C). Finally, it can be shown that little charge is transferred in the FEP/puerarin system, and when the puerarin is replaced by H_2O , one can obtain the largest amount of transferred charge (Figure 4F). As shown in Figure S11, the total number of transferred charges decreases in the system of FEP/puerarin. In summary, as the puerarin concentration increases, the total number of charges transferred between the droplet and the FEP decreases, resulting in a reduction in the electrical signal, as observed experimentally.

2.5 | Structure design and working principle

The TPDS consists of an aluminum foil upper electrode, a FEP friction layer, a Kapton dielectric layers, and an aluminum foil lower electrode. The Kapton, FEP film, and aluminum foil top electrode are cleaned sequentially with

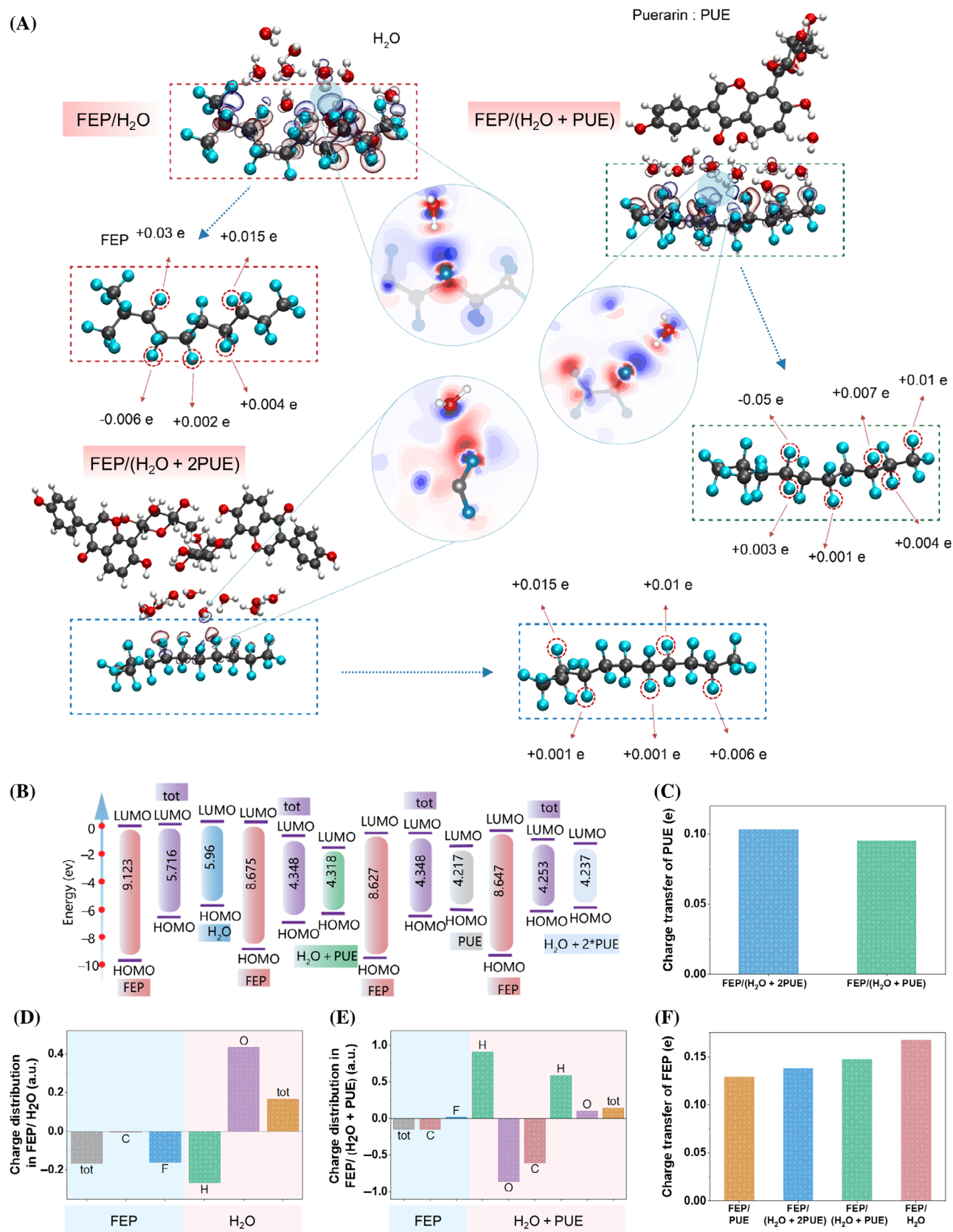


FIGURE 4 Legend on next page.

ethanol and deionized water solution, and then covered with the bottom electrode. When the sensor operates, the top electrode and bottom electrode are electrically connected with a wire, and the sensor operates in the following manner: (i) When there is contact between a droplet and the FEP film, the droplet induces a positive charge, while the FEP film induces a negative charge. (ii) Since FEP is a low-conductivity electret, a layer of negative charge persists on the FEP surface, retaining its intensity for an extended period. This allows for the sustained superposition of the electron cloud as the droplet slides down the FEP layer. (iii) A positive charge is generated on the upper electrode surface, thereby neutralizing the negative charge on the FEP surface. The transfer of electrons occurs from the top electrode to the bottom electrode. (iv) As the droplet moves away from the FEP film, the positive charge is transferred back to the bottom electrode. The movement of electrons is from the bottom electrode to the top. (v) As the droplets repeatedly fall onto the sensor, the charge is continuously transferred between the two electrodes, thereby generating an electrical signal. The magnitude of the signal is proportional to the concentration of puerarin, thereby enabling the detection of concentration. In step “i”, the quantity of charge is contingent upon the concentration of puerarin present in the droplet. The droplet is composed of water and puerarin, where the introduction of puerarin to the droplet results in an enhancement of the transfer of charge from the water to the puerarin, accompanied by a corresponding reduction in the charge interacting with the FEP. Consequently, the electrical signal is observed to be relatively weak when puerarin is present in the droplet. In contrast, the absence of puerarin in the droplet results in the transfer of the entire charge from the water to the FEP, producing a robust electrical signal. In step “ii” the addition of the Kapton film enables the negative friction layer of FEP and the Kapton composite to carry a greater negative charge than the FEP layer alone. This results in an increase in the electric potential energy.

3 | CONCLUSION

In summary, we present a triboelectric puerarin-detecting sensor (TPDS)-based system for detecting the active

ingredient content in natural medicines, which includes a fluorinated ethylene propylene (FEP) friction layer, Kapton dielectric layers, and an upper and lower electrode. This new technology showcases the low cost, ease of use, small size, and rapid response speed, allowing for direct content detection. In addition, the use of the TPDS without an additional power supply or complex circuitry greatly saves on both space and economic costs. This contribution to sustainable development suggests that the TPDS design is capable of meeting diverse challenges related to detection of natural active ingredients.

There is potential for further studies to evaluate the performance of TPDS for future industrial conversion and to assess its resolution and universality to a range of other active ingredients. We have conducted preliminary tests on aqueous extracts of *Astragalus membranaceus* (Fisch) Bge., which showed open-circuit voltages and short-circuit currents of 20 μA and 76 V, respectively (Figure S12), suggesting that the TPDS is versatile for detecting the concentration of other medicinal ingredients. At present, this study has some limitations. First, the hot water extraction method yields numerous active ingredients that are not purified or separated. As a result, the accurate content of puerarin and any similar components cannot be determined individually. Second, if other solvents are used, such as ethanol or n-butanol, it could affect the electron transfer process, altering the size of the electrical signal output. Therefore, the detection process must ensure the solvent's uniqueness and consistency. Last, while the TPDS can measure the trend of the active component content in various solutions, the device's accuracy in detecting solutions with similar concentrations is limited when the concentration of puerarin in solution is greater than 2 $\mu\text{g mL}^{-1}$, making it difficult to determine the specific content. Hence, the device's resolution and precision require improvement, for example by using a more sensitive material for friction or changing the dilution gradient to increase the difference in puerarin concentration in solution.

With its rapid start-up, low cost, and simple pretreatment, the TPDS provides a sustainable and practical approach for converting natural energy into a means of determining the active component content in droplets. This technique holds the potential for widespread use in

FIGURE 4 Charge transfer and interaction analysis of H_2O with different polymers. (A) Charge density difference of Contact Electrification (CE) between FEP and H_2O , the FEP/ H_2O and puerarin (PUE), and the FEP/ H_2O with two molecules of PUE (2PUE); insets indicate the corresponding section map and selected atoms when these different polymers are in contact with water. (B) Simulated frontier orbital energy levels and calculated highest occupied molecular orbital (HOMO)-lowest unoccupied molecular orbital (LUMO) gaps of FEP, H_2O , and PUE diagrams. (C) Change of charge transfer between PUE and H_2O . (D) and (E) Charge distributions in each element and the total charge transfer in the system of FEP/ H_2O , and FEP/(H_2O + PUE), respectively. (F) Total charge transfer in the systems of FEP/ H_2O , FEP/(H_2O + 2PUE), FEP/(H_2O + PUE), and FEP/PUE.

the field of content determination and presents promising possibilities for the portability of such determination.

4 | METHODS

4.1 | Materials and preparation

The commercial Fluorinated Ethylene Propylene (FEP) film was purchased from Shanghai Witlan Industry Co., Ltd; aluminum chloride (AlCl_3 , 99%) was purchased from Shanghai Macklin Biochemical Technology Co., Ltd; sodium hydroxide (NaOH , 90%) was purchased from Shanghai Aladdin Biochemical Technology Co., Ltd.; ferric chloride (FeCl_3 , 98%) was purchased from J&K Scientific; Puerarin (98%) was purchased from Shanghai yuanye Bio-Technology Co., Ltd.

4.2 | Fabrication of TPDS

The structure of the Triboelectric Puerarin Detecting Sensor (TPDS) is composed of a Fluorinated Ethylene Propylene (FEP) film as the friction layer, Kapton as the dielectric layer, and two aluminum electrodes. A laser cutting machine (PLS 4.75, General Laser Systems, USA) was used to cut the right-angled trapezoidal acrylic plate with the upper base of 30 mm, the lower base of 50 mm, the right-angled waist of 20 mm as the column, and the acrylic plate of 50 mm \times 50 mm \times 5 mm as the support layer. Then, a lower electrode made of Al foil, FED, Kapton, and the top electrode made of Al foil is successively covered on the acrylic plate to complete the TPDS.

4.3 | Electrical signal measurement

The electrical output of the TPDS was measured using an Keithley 6514 (Kasley, USA) electrometer. The drop rate was set at 1 drop per second with a drop height of 20 cm, the voltage was measured using a 200 M Ω resistor in parallel to stabilize the baseline voltage.

4.4 | Preparation and detection of solution

The extracted puerarin was diluted 100 times and analyzed using a UV spectrophotometer at a wavelength between 200 and 400 nm. The experimental factors included solid–liquid ratios of 1:10, 1:15, 1:20, 1:25, 1:30, 1:35, 1:40, 1:45, and 1:50; water temperatures of 25, 50,

55, 60, 65, 70, 75, 80, 85, 90, 95, and 100°C; and an extraction time of 1, 2, 3, 4, 5, 6, 7, 8, and 9 min.

4.5 | Qualitative determination of puerarin

Complexation of metal salts: A 5 mL of solution from the Pueraria root was taken and mixed with 1% AlCl_3 solution in a test tube, a yellow-green precipitation appeared in the solution. Reaction with NaOH solution: A 5 mL of solution from Pueraria root was placed in a test tube and mixed with 1 mL of 4% NaOH aqueous solution, the solution turned yellow after mixing. Reaction with FeCl_3 solution: A 5 mL solution of Pueraria root was mixed with a 1% FeCl_3 solution in a test tube, resulting in the solution turning a grassy green color.

4.6 | Detection of puerarin concentration

Standard Curve Creation: To prepare a 50 $\mu\text{g mL}^{-1}$ reserve standard solution, 10 mg of the puerarin standard product was accurately dissolved in distilled water to make a fixed volume of 200 mL. Then, 0, 0.1, 0.2, 0.4, 0.6, 0.8, and 1.0 mL of the solution were accurately measured and distilled water was added to make a total volume of 1 mL. The solution was mixed thoroughly and left to stand for 5 min. Subsequently, the absorbance was measured at 250 nm. Finally, standard curves were produced by plotting the absorbance on the y-axis and the concentration of the standard solution on the x-axis, using the equation provided.

$$A = 0.06752C + 0.10091, R^2 = 0.9941.$$

Here, A represents absorbance and C represents concentration. After determining the extract's absorbance, the puerarin content in the sample was calculated based on the linear regression equation ($n = 3$).

4.7 | Density functional theory (DFT) calculations

DFT calculations were conducted using Gaussian 16. The ground state geometry optimizations and single point energy calculations were carried out through the B3LYP exchange-correlation functional accompanied by the 6-31G** basis set. Grimme's D3 version with the Becke-Johnson damping function was used for conducting the density functional dispersion correction. Atomic dipole

moment corrected Hirshfeld atomic charges (ADCHs) were utilized for estimating the charges.³² The Muliwfn program (version 3.8) was used to analyze the charge density difference, charge transfer, and HOMO–LUMO values.³³

ACKNOWLEDGMENTS

This work was supported by the National Key R & D Project from Minister of Science and Technology in China (No. 2021YFA1201604), the National Natural Science Foundation of China (No. 52072041), the Beijing Natural Science Foundation (Grant No. JQ21007).

CONFLICT OF INTEREST STATEMENT

The authors declare no conflict of interest.

ORCID

Ya Yang  <https://orcid.org/0000-0003-0168-2974>

REFERENCES

1. Fu Z, Chen L, Zhou S, Hong Y, Zhang X, Chen H. Analysis of differences in the accumulation of tea compounds under various processing techniques, geographical origins, and harvesting seasons. *Food Chem.* 2024;430:137000.
2. Zhu Q, Zhou Q, Luo X-L, Zhang XJ, Li SY. Combination of canagliflozin and puerarin alleviates the lipotoxicity to diabetic kidney in mice. *Korean J Physiol Pharmacol.* 2023;27(3):221-230.
3. Cai G, Wu C, Mao N, et al. Isolation, purification and characterization of *Pueraria lobata* polysaccharide and its effects on intestinal function in cyclophosphamide-treated mice. *Int J Biol Macromol.* 2022;218(7):356-367.
4. Qian K, Tan T, Ouyang H, et al. Structural characterization of a homopolysaccharide with hypoglycemic activity from the roots of *Pueraria lobata*. *Food Funct.* 2020;11(8):7104-7114.
5. Van Hung P, Morita N. Chemical compositions, fine structure and physicochemical properties of kudzu (*Pueraria lobata*) starches from different regions. *Food Chem.* 2007;105(2):749-755.
6. Cai G, Wu C, Zhu T, et al. Structure of a *Pueraria* root polysaccharide and its immunoregulatory activity on T and B lymphocytes, macrophages, and immunosuppressive mice. *Int J Biol Macromol.* 2023;230:123386.
7. Li X, Cai W, Lee K, et al. Puerarin attenuates diabetic kidney injury through the suppression of NOX4 expression in podocytes. *Sci Rep.* 2017;7(1):14603.
8. He H, Peng S, Song X, et al. Protective effect of isoflavones and triterpenoid saponins from *Pueraria lobata* on liver diseases: a review. *Food Sci Nutr.* 2022;10(1):272-285.
9. Maciejewska-Turska M, Pecio Ł, Zgórk G. Isolation of mirificin and other bioactive isoflavone glycosides from the kudzu root lyophilisate using centrifugal partition and flash chromatographic techniques. *Molecules.* 2022;27(19):1-13.
10. Fu M, Shah JM, Tang K, et al. Comparative analysis of the medicinal and nutritional components of different varieties of *Pueraria thomsonii* and *Pueraria lobata*. *Front Plant Sci.* 2023;14:1115782.
11. Zhang Y, Xu D, Xing X, Yang H, Gao W, Li P. The chemistry and activity-oriented characterization of isoflavones difference between roots of *Pueraria lobata* and *P. thomsonii* guided by feature-based molecular networking. *Food Chem.* 2023;422:136198.
12. Maji A, Pandit S, Banerji P, et al. *Pueraria tuberosa*: a review on its phytochemical and therapeutic potential. *Nat Prod Res.* 2014;28(23):1-17.
13. Wang J, Yang F, Tao Y, Wang M, Han Z, Zhao H. Phytochemicals and biological activities of *Pueraria* flower: a review. *J Food Bioact.* 2021;13(3):40-51.
14. Wong KH, Li GQ, Li KM, Razmovski-Naumovski V, Chan K. Kudzu root: traditional uses and potential medicinal benefits in diabetes and cardiovascular diseases. *J Ethnopharmacol.* 2011;134(3):584-607.
15. Wang S, Zhang S, Wang S, Gao P, Dai L. A comprehensive review on *Pueraria*: insights on its chemistry and medicinal value. *Biomed Pharmacother.* 2020;131:110734.
16. Miyazawa M, Sakano K, Nakamura S-I, Nakamura SI, Kosaka H. Antimutagenic activity of isoflavone from *Pueraria lobata*. *J Agric Food Chem.* 2001;49(1):336-341.
17. Zhao Y, Xu M, You Z, et al. Analysis of Puerarin and chemical compositions changes in kudzu root during growth period. *J Chem.* 2014;2014:582176.
18. Kim J-S, Woo S-H, Jeong H-M, et al. Component analysis of the Kudzu (*Pueraria lobata*) root and development of Puerarin and starch extraction method. *J Korean Soc Food Sci Nutr.* 2021;51(1):82-86.
19. Choi S, Kim K, Hur N, et al. Effect of heat processing on thermal stability of kudzu (*Pueraria thumbergia* Benth) root isoflavones. *J Life Sci.* 2008;18(10):1447-1454.
20. Xu Z, Talpur Z, Yang W, et al. Dual-spectrum online monitoring of puerarin and total flavonoids contents during the extraction process of *Pueraria lobata*. *Talanta.* 2022;248:123608.
21. Gao Y, Xu M, Wan H, Li C, Wan Y. Determination of Isoflavones in radix puerariae from different origins by ultra-high performance liquid chromatography based on optimal pretreatment method. *Foods.* 2023;12(4):794.
22. Tzanova M, Atanasov V, Yaneva Z, Ivanova D, Dinev T. Selectivity of current extraction techniques for flavonoids from plant materials. *Processes.* 2020;8(10):1222.
23. Wang S, Lin L, Wang ZL. Nanoscale triboelectric-effect-enabled energy conversion for sustainably powering portable electronics. *Nano Lett.* 2012;12(12):6339-6346.
24. Zhang R, Hummelgård M, Örtengren J, et al. All-inorganic triboelectric nanogenerators based on Mo₆S₃I₆ and indium tin oxide. *Nano Energy.* 2021;89:106363.
25. Wei X, Wang B, Cao X, Zhou H, Wu Z, Wang ZL. Dual-sensory fusion self-powered triboelectric taste-sensing system towards effective and low-cost liquid identification. *Nature Food.* 2023;4(8):721-732.
26. Fan C, Wang Q, Chen Y, Ye T, Fan Y. Puerarin from *Pueraria lobata* attenuates ischemia-induced cardiac injuries and inflammation in vitro and in vivo: the key role of miR-130a-5p/HMGB2 pathway. *Chem Biol Drug Des.* 2023;101(4):952-961.
27. Wang D, Bu T, Li Y, He Y, Yang F, Zou L. Pharmacological activity, pharmacokinetics, and clinical research progress of Puerarin. *Antioxidants.* 2022;11(11):2121.

28. Li J, Li Y, Yuan X, et al. The effective constituent puerarin, from *Pueraria lobata*, inhibits the proliferation and inflammation of vascular smooth muscle in atherosclerosis through the miR-29b-3p/IGF1 pathway. *Pharm Biol.* 2022;61(1):1-11.
29. Yue S, Zhou R, Nan T, et al. Comparison of major chemical components in *Puerariae Thomsonii* radix and *Puerariae Lobatae* Radix. *China J Chin Mater Med.* 2022;47(10):2689-2697.
30. Thapa P, Kim H, Hong JP, et al. Absolute quantification of isoflavones in the flowers of *Pueraria lobata* by qHNMR. *Plan Theory.* 2022;11(4):548.
31. Wang Y, Yang Y, Sun H, et al. Application of a data fusion strategy combined with multivariate statistical analysis for quantification of puerarin in Radix puerariae. *Vib Spectrosc.* 2020;108:103057.
32. Lu T, Chen F. Atomic dipole moment corrected Hirshfeld population method. *J Theor Comput Chem.* 2012;11(1):163-183.
33. Lu T, Chen F. Multiwfn: a multifunctional wavefunction analyzer. *J Comput Chem.* 2012;33(5):580-592.

SUPPORTING INFORMATION

Additional supporting information can be found online in the Supporting Information section at the end of this article.

How to cite this article: Su C, Shao J, Yu Z, et al.

Miniature and cost-effective self-powered triboelectric sensing system toward rapid detection of puerarin concentration. *InfoMat.* 2024;e12624.

doi:[10.1002/inf2.12624](https://doi.org/10.1002/inf2.12624)